Effect of an equilibrium phase transition on multiphase transport in relativistic heavy ion collisions

Yu Meiling,* Du Jiaxin, and Liu Lianshou†
Institute of Particle Physics, Huazhong Normal University, Wuhan 430079, People's Republic of China
(Received 14 June 2006; published 30 October 2006)

The hadronization scheme for parton transport in relativistic heavy ion collisions is considered in detail. It is pointed out that the traditional scheme for particles being freezed out one by one leads to serious problem on unreasonable long lifetime of partons. A collective phase transition following a supercooling is implemented in a simple way. It turns out that the modified model with a sudden phase transition is able to reproduce the experimental longitudinal distributions of final state particles better than the original one does. The encouraging results indicate that equilibrium phase transition should be taken into proper account in parton transport models for relativistic heavy ion collisions.

DOI: 10.1103/PhysRevC.74.044909 PACS number(s): 25.75.−q, 12.38.Mh, 24.10.Lx

I. INTRODUCTION

The quark-gluon plasma (QGP) is expected to be formed in heavy-ion collisions at the Relativistic Heavy-Ion Collider (RHIC). So far very interesting experimental data have been collected [1]. There are strong evidences on the deconfinement of QCD vacuum and the appearance of a (locally) thermalized partonic system at the early stage of collision. Both theoretical and experimental investigations are stimulated on the evolution of the partonic system and the way it transforms to final state particles.

The reaction process of relativistic heavy ion collision can be divided into several stages (see Fig. 1). At first the primary interaction creates many partons. These partons are certainly far from equilibrium and cascade through the interactions among them. If the colliding nuclei is heavy enough and the incident energy is high enough, the partonic system is expected to reach equilibrium or local equilibrium, forming quark-gluon plasma (QGP). The system then expands and the temperature decreases, passing via a phase transition or crossover into the hadron gas (HG) stage. Hadrons continue to cascade until they freeze-out from the collision region, forming final state particles.

At present there is no unique theory that can describe the reaction process as a whole. Different theoretical approaches are applied to different stages [2]. The primary interaction, creating many partons is often described by eikonalized parton model [3], Gribov-Regge theory [4] or parton saturation model [5]. Parton and/or hadron cascade is referred to as the solution of nonequilibrium transport equation [6] and is usually realized by Monte Carlo models [7–9]. The hydrodynamics [10] or thermal models [11] are employed to deal with the parton and/or hadron system in local or global equilibrium.

Usually, the hydrodynamics or thermal models take (local) equilibrium as model assumption and do not answer the question on how the system arrives at (local) equilibrium. The global properties of the system are the main issues considered in the model, while the detailed evolution of the constituents—partons and/or hadrons is not taken into account.

On the contrary, the transport models simulate the evolution of the partons and/or hadrons in detail through considering their interactions—elastic and/or inelastic scattering or cascade. Usually, this kind of models allow the cascade to continue until the interactions cease and then the partons or hadrons freeze-out from the system. A noticeable common property of such models is that, each particle has its own freeze-out time and the partons or hadrons freeze-out one by one. Such an approach is acceptable for a hadronic system, where hadrons after ceasing interaction fly away from the system freely toward the detectors, but causes serious problem for a partonic system.

Partonic and hadronic systems are of different phases, existing in different vacua—the former is in the perturbation QCD vacuum and the latter in the physical vacuum. Therefore, the transition between partonic and hadronic phases should be a collective phenomenon, accompanied by a vacuum transform, which could not be realized in a particle-by-particle way.

In the transport models presently on market, the hadronization is realized parton-wise instead of collectively, and therefore, in these models there is only *hadronization* but no partonic to hadronic *phase transition* in the strict sense. To let a few partons live for a very long time is inconsistent with the general believe that the existing time of QGP is about 1–5 fm/*c* [12] and hadron freeze-out at about 20–40 fm/*c* [13]. Even more seriously, when most of the partons have already hadronized, the system is dominated by hadrons, which corresponds to a physical vacuum instead of a QCD perturbation one. It is unphysical to let some partons survive and fly freely in such a circumstance.

The aim of the present paper is to discuss this problem in detail. We will take as example a presently available model—a multiphase transport model (AMPT) [9], where parton transport has been implemented. The temperature of the system at different time will be extracted using thermal-equilibrium transverse mass distribution. The partonic system will be allowed to be somewhat *super-cooled*, i.e., the temperature

*Email address: yuml@iopp.ccnu.edu.cn
†Email address: liuls@iopp.ccnu.edu.cn

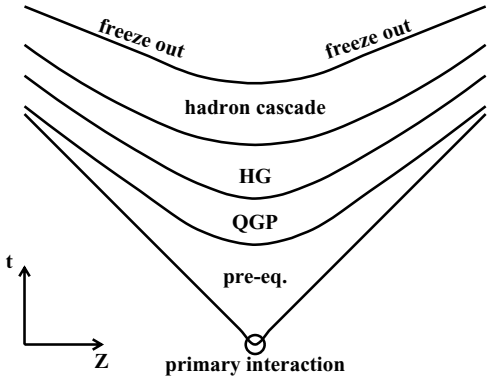

FIG. 1. The different stages of heavy-ion collisions.

is able to decrease to lower than the expected phase transition temperature. At a certain point all the partons remaining in the system are forced to coalesce suddenly, forming hadrons. Then the hadrons start to cascade toward freeze out. Thus the problem of unphysical *long-life partons* is solved in a simple manner. The phenomenological consequences of such an approach will be presented and compared with existing experimental data. The possible reason for the improvement of the present approach with collective hadronization in comparison with the original model with long-life partons will be discussed.

The layout of the paper is as follows. A short introduction to the AMPT model is given in Sec. II. A detailed analysis about the parton and hadron time evolution in AMPT is then presented in Sec. III. A collective hadronization scheme following a super-cooling of the parton system is proposed in Sec. IV together with the phenomenological consequences on the final hadron distribution and elliptic flow. Section V is conclusion and discussion.

II. A BRIEF INTRODUCTION TO AMPT

The AMPT model is based on nonequilibrium transport dynamics. It contains four main components: the initial conditions, partonic interactions, conversion from the partonic to the hadronic matter and hadronic interactions. The initial conditions, which includes the spatial and momentum distributions of minijet partons from hard processes and strings from soft processes, are obtained from the heavy ion jet interaction generator HIJING [3]. This is a Monte Carlo event generator for hadron-hadron, hadron-nucleus, and nucleus-nucleus collisions. In this model, the radial density profiles of the two colliding nuclei are taken to have Woods-Saxon shapes, and multiple scattering among incoming nucleons are treated in the eikonal formalism. Particle production from two colliding nucleons is described in terms of a hard and a soft component. The hard processes lead to the production of energetic minijet partons and is simulated by PYTHIA program. The soft component, on the other hand, takes into account nonperturbation process and is simulated by the formation of strings.

After the primary interactions, the time evolution of partons is then treated according to the Zhang's parton cascade (ZPC) model [14]. At present this model includes only parton-parton elastic scattering with cross section

$$\sigma_p \simeq \frac{9\pi\alpha_s^2}{2\mu^2}, \tag{1}$$

where the screening mass μ is taken to be an input parameter of the model to obtain the desired total cross section. Two partons will undergo scattering when the closest distance between them is smaller than $\sqrt{\sigma/\pi}$.

There are two versions of AMPT model. In the default AMPT (v1.11), after ceasing interactions minijet partons are combined with their parent strings to form excited strings, which are then converted to hadrons according to the Lund string fragmentation model. While in the AMPT with string melting (v2.11), the strings in the initial conditions are melted to partons first and then interactions among all the partons are again simulated by Zhang's parton cascade model. After partons stop interacting, a simple quark coalescence model is used to combine the two nearest partons into a meson and three nearest quarks (antiquarks) into a baryon (antibaryon).

Scattering among the resulting hadrons are described by a relativistic transport (ART) model [15] which includes baryon-baryon, baryon-meson and meson-meson elastic and inelastic scattering.

It turns out that the default AMPT (v1.11) is able to give a reasonable description on hadron rapidity distributions and transverse momentum spectra observed in heavy ion collisions at both SPS and RHIC. However, it fails to reproduce the experimental data about elliptic flow and two-pion correlation function. On the other hand, the AMPT model with string melting (v2.11) can well describe the elliptic flow and two-pion correlation function [16,17] but agrees badly with the hadron rapidity and transverse momentum spectra.

In the following we will utilize the AMPT v2.11 to generate Au-Au central collision events at $\sqrt{s_{NN}} = 200$ GeV. The impact parameter is in the range $b \leqslant 3$ fm and the parton cross section is taken to be 10 mb.

III. THE TIME EVOLUTION OF PARTONS AND HADRONS IN AMPT

In AMPT v2.11, each initial parton has a formation time given by $t_f = E_H/m_{T,H}^2$ with $E_H, m_{T,H}$ the energy and transverse mass of its parent hadrons, respectively. After this formation time the partons start to scatter with each other. When a parton no longer scatters with any other parton, it will freeze-out—hadronize. Thus each parton has its own hadronization time.

In Fig. 2 are shown the percentages of parton and hadron, respectively, at different time after the collision. It can be seen from the figure that a few hadrons (about 4%) have already emerged at $t < 5$ fm/c. At this time, partons dominate, and the system as a whole is in the deconfined phase, located in the perturbation QCD vacuum, with a few hadrons vaporized out.

As time increases, the number of partons decreases while that of hadrons increases. In this process a parton transforms to hadron when and only when it ceases to interact with other partons. Thus a part of parton survive up to an unreasonable long time, e.g., $t \sim 100$ fm/c. This is the common defect for this kind of models mentioned in the Introduction.

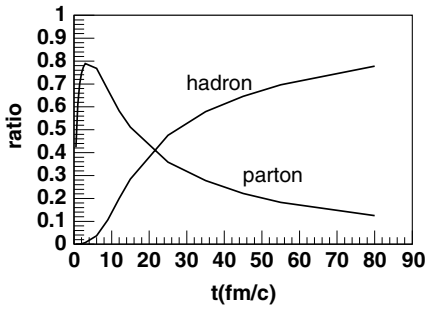

FIG. 2. The percentage of partons and hadrons, respectively, in AMPT v2.11 for $\sqrt{s_{NN}} = 200$ GeV Au-Au central collisions with $b \leqslant 3$ fm and parton cross section 10 mb.

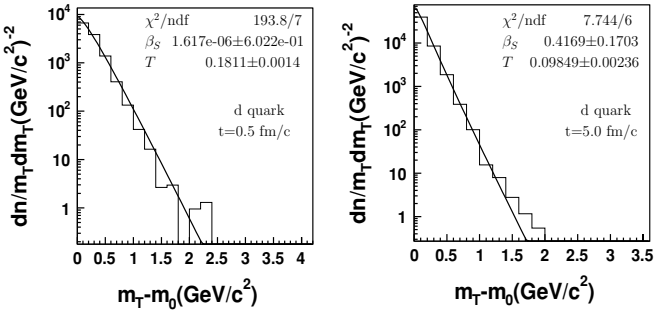

FIG. 3. The transverse mass distribution (histograms) for d-quarks at two different times $t = 0.5$ and 5 fm/c. The lines are the fit to Eq. (3).

To study the phase transition from partons to hadrons, we need to know the time evolution of the local temperature. We assume the system is locally thermal equilibrated. Under this assumption a thermal + transverse radial flow model [18] is used to extract the temperature of the system at different time. In this model the invariant momentum spectrum of particles emitted from the given isotherm $\sigma(r, \phi, \zeta)$ is given by

$$E\frac{d^3n}{d^3p} = \int_\sigma f(x, p)p^\lambda d\sigma_\lambda \simeq \frac{g}{(2\pi)^3}\int e^{-(u^\nu p_\nu - \mu)/T} p^\lambda d\sigma_\lambda, \tag{2}$$

where $f(x, p)$ is the invariant distribution function, which is assumed to be an anisotropic thermal distribution boosted by the local fluid velocity u^μ. Integrating with respect to ϕ and ζ, we get the transverse mass distribution

$$\frac{dn}{m_T dm_T} \propto m_T \int_0^R r dr K_1\left(\frac{m_T \cosh\rho}{T}\right) I_0\left(\frac{p_T \sinh\rho}{T}\right) \tag{3}$$

in which I_0 and K_1 are modified Bessel functions, T is the kinetic freeze-out temperature, and $\rho = \tanh^{-1}\beta_r(r)$ is the boost rapidity. $\beta_r(r)$ is the transverse velocity distribution in the region $0 < r < R$, which has a self-similar profile parameterized by the surface radial velocity β_S:

$$\beta_r(r) = \beta_S\left(\frac{r}{R}\right)^\alpha. \tag{4}$$

The exponent α describes the evolution of the flow velocity. Through fitting the transverse mass distribution with four parameters—α, T, β_S, and a normalization factor, the surface radial velocity β_S and the temperature T of the system can be extracted.

IV. A COLLECTIVE PHASE TRANSITION FOLLOWING A SUPERCOOLING

As an example, in Fig. 3 are shown the transverse mass distributions for d quarks at two different times $t = 0.5$ and 5 fm/c and the fit to Eq. (3). It can be seen from the figure that the temperature of the parton system is about 180 MeV at $t = 0.5$ fm/c, slightly above the predicted critical temperature $T_c = 170$ MeV [19], while at $t = 5$ fm/c the temperature has already arrived at about 100 MeV, i.e., in the first few fm/c the temperature decreases rapidly and soon becomes lower than the expected phase transition temperature.

We regard the temperature of parton system decreasing rapidly to lower than the critical temperature as a *supercooling effect* [20], i.e., after the formation of QGP, the system lowers its temperature through expanding and evaporating hadrons, arriving at a temperature lower than the critical one. Then at a certain point all the left partons are coalesced to hadrons. The duration of the supercooling state is taken as a model parameter and in the present work we take $t = 5$ fm/c (the corresponding parton temperature is about 100 MeV) to be the beginning of the phase transition. At this time, all the remaining partons stop interacting and start to hadronize. The temperature of the resulting hadron system is higher than that of the parton system due to the release of latent heat, and then the temperature decreases again through expanding, cf. Figs. 4 and 5.

In Fig. 4 is shown the time dependence of the surface radial velocity β_S of hadrons extracted from the fitting to pion invariant transverse mass spectra by Eq. (3) for the model with phase transition. In Fig. 5 is presented the temperature of the system extracted from parton (d quark) and hadron (pion) invariant transverse mass distributions at different time by Eq. (3) for the model with phase transition.

From the figures it can be seen that a small amount of hadron vaporize from the parton system already at a high temperature

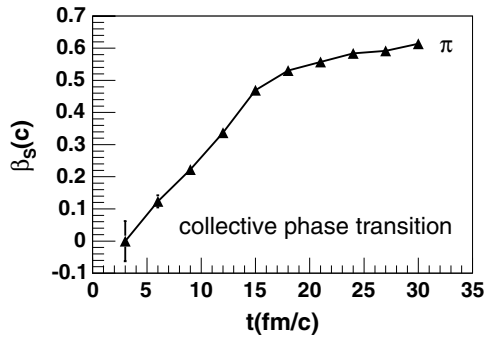

FIG. 4. The surface radial velocity extracted from hadron transverse mass spectra in AMPT v2.11 with a sudden phase transition implemented at $t = 5$ fm/c for $\sqrt{s_{NN}} = 200$ GeV Au-Au central collisions with $b \leqslant 3$ fm and parton cross section 10 mb.

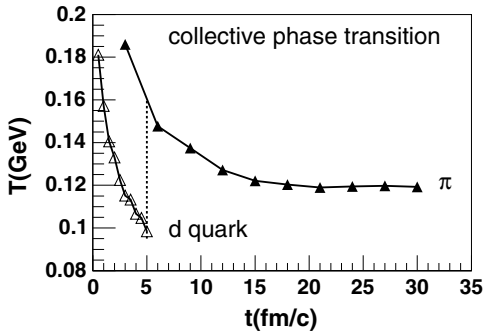

FIG. 5. The temperature evolution extracted from parton and hadron transverse mass spectra in AMPT v2.11 with a sudden phase transition implemented at $t = 5$ fm/c for $\sqrt{s_{NN}} = 200$ GeV Au-Au central collisions with $b \leqslant 3$ fm and parton cross section 10 mb.

before $t = 5$ fm/c. After the sudden phase transition, the resulting hadron system expands with surface radial velocity β_S. At first the expanding velocity increases rapidly with time and then gradually slowing down, cf. Fig. 4. After t arrives about 15 fm/c, the expanding radial velocity of the system changes only slightly with time, leading to a nearly flat distribution of system temperature as shown in Fig. 5.

Thus we have implemented a collective phase transition following a supercooling to the transport model in a very simple way. Our purpose is to see how the phase transition affects the final state hadron distributions.

The rapidity distribution is

$$\frac{dN}{dy} = \frac{1}{\mathcal{N}_{\rm ev}} \frac{\Delta n}{\Delta y}, \tag{5}$$

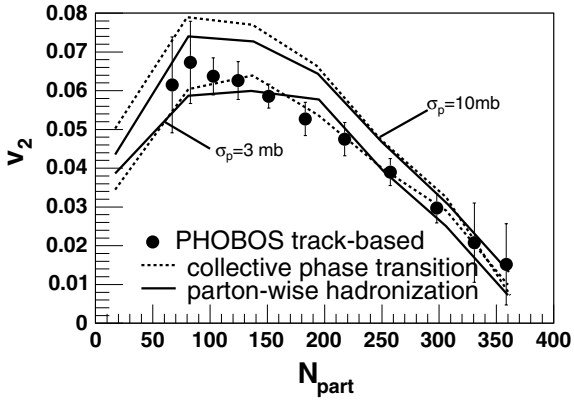

FIG. 7. Centrality dependence of charged hadron elliptic flow for $\sqrt{s_{NN}} = 200$ GeV Au-Au central collisions. The solid lines are the AMPT v2.11 with parton-wise hadronization and dashed lines are that with sudden phase transition implemented. The dots are data from PHOBOS experiments [24]. The impact parameter $b \leqslant 3$ and parton cross section is 10 mb and 3 mb, respectively.

where $\mathcal{N}_{\rm ev}$ is the number of events, Δy is the width of rapidity bin, Δn is the number of particles inside the rapidity bin. In Fig. 6, the rapidity distributions for charged particles, pions, kaons, net-protons, protons and antiprotons are shown. The solid lines represent the results of AMPT v2.11 with parton-wise hadronization and the dotted lines are that with a sudden phase transition implemented in the above mentioned way. Full circles are PHOBOS [21] 0%–6% centrality data and BRAHMS [22,23] 0%–5% centrality data. The data of $dN_{\rm ch}/d\eta$ are with both statistical and systematic errors and the other data are with only statistical ones. The figures show that the rapidity distributions of the model with phase

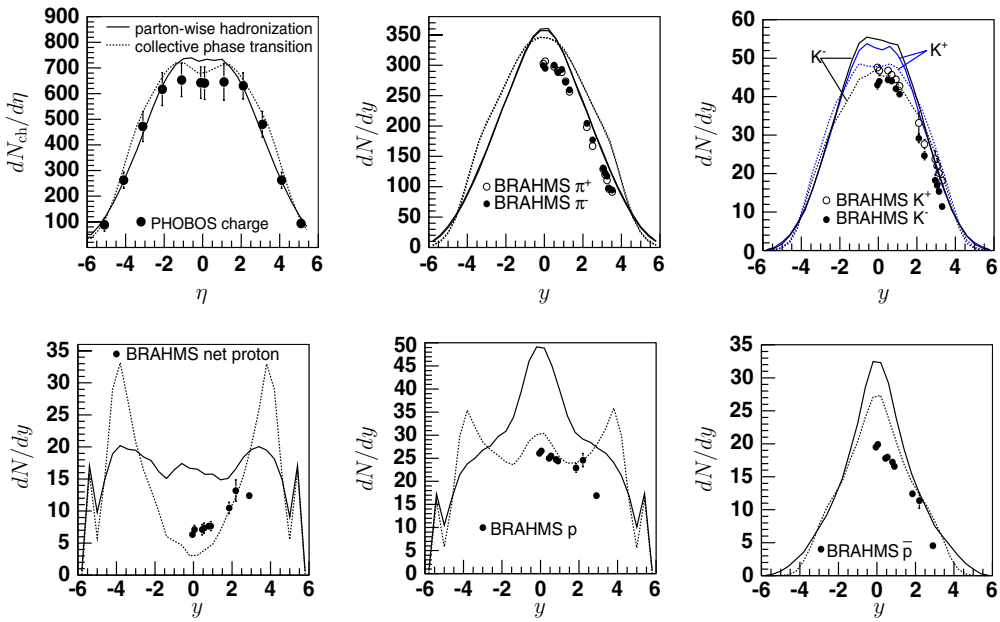

FIG. 6. (Color online) The rapidity distribution for $\sqrt{s_{NN}} = 200$ GeV Au-Au central collisions. The solid lines are AMPT v2.11 with parton-wise hadronization and the dashed lines are that with sudden phase transition implemented. The impact parameter is $b \leqslant 3$ and parton cross section 10 mb. The dots are data from PHOBOS 6% and BRAHMS 5% central collisions.

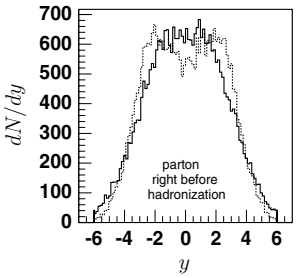

FIG. 8. The rapidity distribution of partons right before hadronization in AMPT v2.11 with parton-wise hadronization (solid line) and with collective phase transition (dashed line.)

transition implemented describes the experimental data better, especially for the kaon and proton rapidity distributions. As about the transverse distributions we found that they are almost unaffected by the implementation of collective phase transition.

The success of AMPT with string melting is that it is able to describe the elliptic flow data very well through adjusting the parton cross section. So, whether the implementation of a sudden phase transition will destroy the agreement between model and data is a natural question.

In Fig. 7 is shown the elliptic flow v_2 as a function of the number of participants calculated from the AMPT (with string melting) model with parton-wise hadronization and with collective phase transition, respectively. The parton cross sections are taken to be 3 mb and 10 mb. It is clear from the figure that the v_2 with sudden phase transition implemented has almost the same shape as that with parton-wise hadronization. The implementation of collective phase transition affects the elliptic flow little and preserves the agreement between model and experimental data.

V. CONCLUSION AND DISCUSSION

In the traditional transport models the particles in the system are freezed out one by one with individual freeze-out time. Extending such an approach to parton transport leads to serious problem on unreasonable long lifetime for partons.

In order to avoid this problem, we assume the system to have reached local equilibrium and extract temperature from the system by thermodynamics formula. As the decreasing of temperature the parton phase is allowed to hadronize as a whole after a supercooling stage. It turns out that the modified model with a sudden phase transition inherits the success of the original one in elliptic flow and is able to reproduce the experimental longitudinal distributions of final state particles better than the original one does.

In order to see why the model with collective hadronization can describe the experimental data better, the rapidity distributions of partons right before hadronization are plotted in Fig. 8. Compared to the model with parton-wise hadronization, the parton transport in the model with sudden phase transition is truncated, so there are fewer partons in the mid-rapidity region and the distribution peaks at regions with large absolute values of rapidity. This effect results in lower hadron distribution in the mid-rapidity region than that from the original model, which makes the distribution of the final state hadrons closer to the experimental data.

The elliptic flow in parton cascade model is built-up very early [16,25] (less than 5 fm/c), thus the truncation of parton transport at 5 fm/c in the present work does not affect the elliptic flow.

We have proposed a collective hadronization following a supercooling as a prototype of the thermal-equilibrium phase transition from parton transport to hadron gas. Though our method for the implementation of phase transition seems to be very crude comparing to the real process in relativistic heavy ion collisions, the encouraging results indicate that a relevant parton transport model for relativistic heavy ion collision should take equilibrium phase transition into proper account.

ACKNOWLEDGMENTS

This work was supported in part by the National Science Foundation of China under project 10375025 and by the Cultivation Fund of the Key Scientific and Technical Innovation Project, Ministry of Education of China No. CFKSTIP-704035.

[1] J. Adams *et al*. (STAR Collaboration), Nucl. Phys. **A757**, 102 (2005); K. Adcox *et al*. (PHENIX Collaboration), *ibid*. **A757**, 184 (2005).
[2] K. Werner, J. Phys. G: Nucl. Part. Phys. **27**, 625 (2001).
[3] X.-N. Wang, Phys. Rev. D **43**, 104 (1991); M. Gyulassy and X. N. Wang, Comput. Phys. Commun. **83**, 307 (1994).
[4] K. Werner, Phys. Rep. **232**, 87 (1993).
[5] L. McLerran and R. Venugopalan, Phys. Rev. D **49**, 2233 (1994); K. J. Eskola, K. Kajantie, P. V. Ruuskanen, and K. Tuominen, Phys. Lett. **B543**, 208 (2002).
[6] H. Sorge, H. Stocker, and W. Greiner, Nucl. Phys. **A498**, 567c (1989); Y. Pang, T. J. Schlagel, and S. H. Kahana, Phys. Rev. Lett. **68**, 2743 (1992).
[7] H. Sorge, Phys. Rev. C **52**, 3291 (1995).
[8] S. A. Bass *et al*., Prog. Part. Nucl. Phys. **41**, 225 (1998), also see nucl-th/9803035.
[9] Z. W. Lin, C. M. Ko, B. A. Li, B. Zhang, and S. Pal, Phys. Rev. C **72**, 064901 (2005); Z. W. Lin, S. Pal, C. M. Ko, B. A. Li, and B. Zhang, *ibid*. **64**, 011902(R) (2001); B. Zhang, C. M. Ko, B. A. Li, and Z .W. Lin, *ibid*. **61**, 067901 (2000).
[10] C. M. Hung and E. V. Shuryak, Phys. Rev. Lett. **75**, 4003 (1995); P. F. Kolb, U. W. Heinz, P. Huovinen, K. J. Eskola, and K. Tuominen, Nucl. Phys. **A696**, 197 (2001).
[11] P. Braun-Munzinger, J. Stachel, J. P. Wessels, and N. Xu, Phys. Lett. **B344**, 43 (1995); F. Becattini, J. Cleymans, A. Keranen, E. Suhonen, and K. Redlich, Phys. Rev. C **64**, 024901 (2001).
[12] T. S. Biro, E. van Doorn, B. Müller, M. H. Thoma, and X.-N. Wang, Phys. Rev. C **48**, 1275 (1993).
[13] L. P. Csernai and J. I. Kapusta, Phys. Rev. D **46**, 1379 (1992); Phys. Rev. Lett. **69**, 737 (1992).
[14] B. Zhang, Comput. Phys. Commun. **109**, 193 (1998).
[15] B. A. Li and C. M. Ko, Phys. Rev. C **52**, 2037 (1995).

[16] Z.-W. Lin and C. M. Ko, Phys. Rev. C **65**, 034904 (2002).
[17] Z.-W. Lin, C. M. Ko, and S. Pal, Phys. Rev. Lett. **89**, 152301 (2002).
[18] E. Schnedermann, J. Sollfrank, and U. Heinz, Phys. Rev. C **48**, 2462 (1993).
[19] F. Karsch, Lect. Notes Phys. **583**, 209 (2002); E. V. Shuryak, Phys. Rev. Lett. **68**, 3270 (1992).
[20] J. Kapusta and A. Mekjian, Phys. Rev. D **33**, 1304 (1986); T. Csorgo and L. P. Csernai, Phys. Lett. **B333**, 494 (1994); T. De Grand and K. Kajantie, *ibid.* **B147**, 273 (1984).
[21] B. B. Back *et al*. (PHOBOS Collaboration), Phys. Rev. Lett. **91**, 052303 (2003).
[22] I. G. Bearden *et al*. (BRAHMS Collaboration), Phys. Rev. Lett. **94**, 162301 (2005).
[23] I. G. Bearden *et al*. (BRAHMS Collaboration), Phys. Rev. Lett. **93**, 102301 (2004).
[24] B. B. Back *et al*. (PHOBOS Collaboration), Phys. Rev. C **72**, 051901(R) (2005).
[25] B. Zhang, M. Gyulassy, and C. M. Ko, Phys. Lett. **B455**, 45 (1999).